

OBP-LLM: Optimizing Boundary Perception of Large Language Model for Few-shot NER

Anonymous ACL submission

Abstract

Few-shot Named Entity Recognition (NER) enables models to learn effectively from limited annotated samples and perform robustly, even in resource-rich domains, addressing the challenge of scarce labeled data in many fields. Recently, Large Language Models (LLMs) have demonstrated strong adaptability and generalization capabilities in few-shot learning, offering new solutions for few-shot NER tasks. In this paper, we propose OBP-LLM, a novel large language model-based method that integrates contrastive learning and Direct Preference Optimization (DPO) to address attention mismatch and generation fallacy in LLM-based NER, by refining internal attention and generation preferences. Experimental results demonstrate that our method significantly outperforms existing approaches on multiple Few-shot NER benchmarks, including Few-NERD and CrossNER, particularly in cross-domain and extremely low-resource scenarios. This study validates the potential of contrastive learning and DPO in optimizing LLMs and provides new directions and practical solutions for NER tasks in low-resource domains.

1 Introduction

Named Entity Recognition (NER) is a critical task in natural language processing closely related to numerous other tasks. It aims to extract entities from unstructured text and classify them into pre-defined categories, such as person names, location names, and organization names (Guo et al., 2009; Mollá et al., 2006; Nadeau and Sekine, 2007). In recent years, deep learning models have achieved significant progress in NER tasks, particularly supervised methods based on pre-trained models like BERT (Devlin et al., 2019) and RoBERTa (Liu et al., 2019), which achieve high accuracy by training on large-scale annotated datasets. However, these traditional methods heavily rely on extensive manually annotated datasets, which are often costly

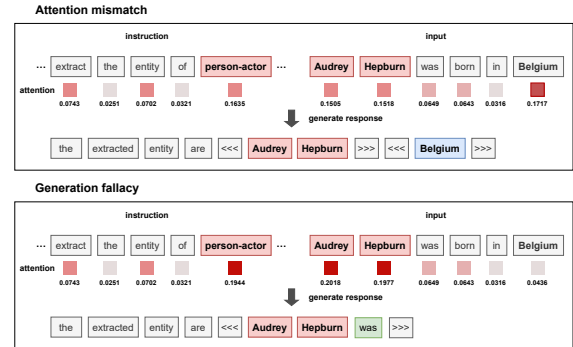


Figure 1: An illustration of two challenges applying the text generation framework of large language models to NER tasks. Here, we use Llama3.1-8b as the base model and compute the average of all multi-head attention scores at the 26th layer.

and time-consuming to obtain. Additionally, they exhibit limited flexibility in cross-domain applications. To address these issues, Few-shot Learning (FSL) (Ding et al., 2021a; Huang et al., 2021) has emerged as a research focus on NER tasks. The strength of FSL is its capability to identify new categories with few annotated samples, reducing the need for large labeled datasets while greatly enhancing cross-domain adaptability.

Existing few-shot NER methods generally follow two paradigms:

- (1) **one-stage**: Reformulates NER task as sequence labeling via prototypical networks, classifying tokens based on distances to class prototypes.
- (2) **two-stage**: Splits NER task into span extraction and entity classification.

With the rise of generative Large Language Models (LLMs), Few-shot NER tasks have seen breakthroughs. Compared to traditional pre-trained models, LLMs, such as Llama-3 (Dubey et al., 2024) and GPT-4 (Achiam et al., 2023), have larger parameter scales and stronger generalization capabilities. By designing various prompts, LLM can efficiently perform diverse NLP tasks without fine-tuning, demonstrating exceptional performance in

few-shot learning scenarios (Zhang et al., 2024). We adopt a one-stage approach to avoid the error propagation issues commonly associated with the two-stage paradigm. However, we find that applying the text generation framework of LLMs to one-stage NER tasks still suffers from two major limitations (shown in Figure 1). 1) **Attention mismatch**: Input text suffers from attenuated attention allocation within the prompt, causing the model to focus on irrelevant tokens during response generation. 2) **Generation fallacy**: Although the model’s attention is focused on the correct tokens, errors still occur during generation (e.g., incorrect entity boundaries).

To address these limitations, we propose a novel framework for LLMs based on contrastive learning and Reinforcement Learning, enhancing the model’s perception of entity boundaries to ensure the generation of accurate entity responses. This framework achieves exceptional performance in extremely low-resource named entity recognition tasks by fine-tuning only a subset of LLM parameters via the LoRA method (Hu et al., 2021).

On the one hand, we impose constraints on the decoding phase during response generation, ensuring that generated tokens are derived solely from the input text. Additionally, we introduce attention-based contrastive learning during the Supervised Fine-Tuning (SFT) stage, bringing entities of the same category closer together while pushing different categories further apart in the semantic space. This optimization refines the distribution of entity representations, enabling a global semantic adjustment that enhances local attention mechanisms, thereby guiding the model to focus on the correct tokens.

On the other hand, to retain the rich boundary information utilized in two-stage methods without task decomposition (which risks cascading errors from subtasks), we construct preference data based on entity boundaries and error feedback from the initially aligned model. Through reinforcement learning, the model learns more precise boundary information and corrects previous errors to some extent. To simplify the reinforcement learning process, we adopt the computationally efficient Direct Preference Optimization (DPO) approach (Rafailov et al., 2023). Extensive experiments across multiple benchmarks demonstrate that our method consistently outperforms existing state-of-the-art approaches.

In summary, our main contributions are as fol-

lows:

(1) We propose a novel large language model-based approach to address few-shot NER tasks, which requires training only a subset of parameters yet demonstrates strong generalization capabilities on novel entity categories, especially in scenarios with extremely limited training samples.

(2) We address the attention mismatch and generation fallacy issues inherent in applying LLM-based generation to one-stage NER. To this end, we incorporate contrastive learning to enhance entity semantics and guide attention to relevant tokens, and apply Direct Preference Optimization (DPO) to enrich boundary perception and enable self-correction from error feedback, ensuring more accurate generation.

(3) Experiments conducted on two widely used few-shot NER benchmarks demonstrate that our method outperforms current state-of-the-art approaches, particularly in more challenging tasks.

2 Related Work

2.1 Few-shot Named Entity Recognition

Few-shot Named Entity Recognition (NER) aims to efficiently identify and classify entities with limited annotated data. The primary challenge is learning robust entity representations and achieving strong generalization under data scarcity.

One-stage methods (Fritzler et al., 2019; Gao et al., 2019; Yang and Katiyar, 2020; Hou et al., 2020; Ma et al., 2022a) transform NER tasks into sequence-labeling problems using prototype networks, classifying tokens by computing their distance to category prototypes. While computationally efficient, they are susceptible to interference from the non-entity label "O," degrading classification performance. Moreover, in transformer-based pre-trained models like BERT, self-attention mechanisms can cause cross-entity interference within the same sentence, leading to densely packed or overlapping entity distributions in the semantic space.

Two-stage methods (Shen et al., 2021; Wang et al., 2022b; Ma et al., 2022b; Wang et al., 2022a; Dong et al., 2023; Guo et al., 2024) methods decompose NER tasks into two independent processes—span extraction and entity classification. The model first extracts all potential entity spans without assigning categories, followed by classification for each candidate span. While this decomposition improves entity boundary modeling,

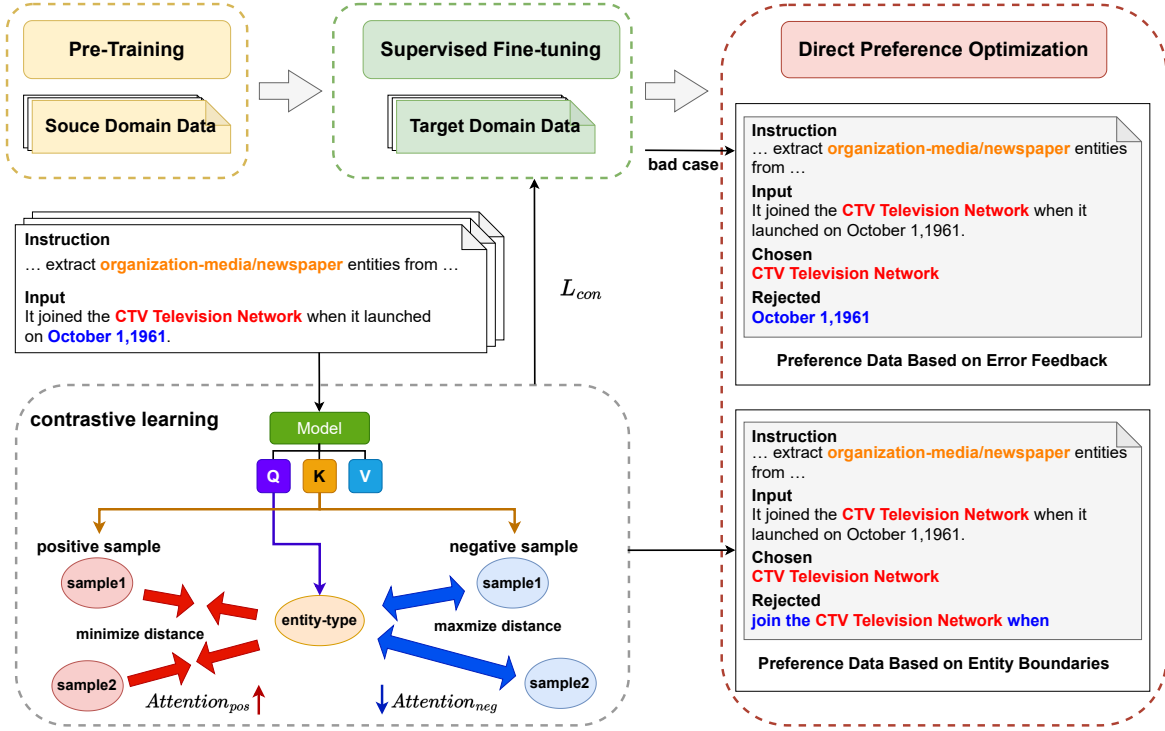


Figure 2: The overall architecture of OBP-LLM. It consists of three stages: pre-training on the source domain, supervised fine-tuning on the target domain, and Direct Preference Optimization.

performance heavily depends on span extractor accuracy. Errors in span extraction inevitably impact entity classification.

Furthermore, with the recent emergence of LLMs demonstrating remarkable capabilities in few-shot learning, several works have explored applying LLMs to few-shot NER tasks (Wang et al., 2023; Zhu et al., 2024).

2.2 Contrastive learning

The foundational concept of contrastive learning lies in the analysis of feature similarities and disparities. Hadsell et al. (2006) introduced contrastive loss, which refines feature representations by minimizing the distance between positive pairs while maximizing the separation between negative pairs. In recent years, contrastive learning has seen rapid advancements, particularly in computer vision and natural language processing (Chen et al., 2020; He et al., 2020). Today, contrastive learning has become a cornerstone technique in pre-training, finding widespread application (Reimers, 2019; Gao et al., 2021).

2.3 Direct Preference Optimization

Reinforcement Learning from Human Feedback (RLHF) optimizes model behavior by incorporating human preferences to align generated content

with user expectations. Christiano et al. (2017) applied RLHF to simulated games and simple text generation tasks, while Ziegler et al. (2019) used human feedback to enhance the quality, coherence, and style of language model outputs, demonstrating its effectiveness in task optimization.

With the rise of pre-trained language models (e.g., the GPT series), RLHF has been widely adopted to improve text generation quality and control (Stiennon et al., 2020). The introduction of InstructGPT (Ouyang et al., 2022) and ChatGPT marks a key milestone in its application, driving its expansion in large-scale language models.

3 Method

3.1 Prompt Construction

Before starting the training process, we first construct a prompt for the LLM to adapt to the NER task (Zhang et al., 2024). Figure 3 below provides an example of such a prompt, which consists of four parts: (1) The first line is a fixed description of the alpaca-lora method, introducing the following three sections: Instruction, Input, and Response. (2) instruction: In this part, we specify the entity categories to be extracted and briefly describe the definition of each entity type to help the LLM better understand the NER task. (3) input: The sen-

Below is an instruction that describes a task, paired with an input that provides further context. Write a response that appropriately completes the request.

instruction: I want you to extract **organization-media/newspaper** entities from the following input sentence, the entity of **organization-media/newspaper** refers to the entity that represents a specific media outlet, newspaper, or press organization in the input sentence.

input: It joined the **CTV Television Network** when it launched on October 1, 1961.

response: The entities I extracted for you are <<< **CTV Television Network** >>> .

Figure 3: a example of prompt

tence from which entities are to be extracted. (4) response: This section contains the model’s generated output, where each extracted entity is enclosed within <<< >>> identifiers.

3.2 Pre-Training in Source Domain

We first construct training data from the source Domain using the prompt designed in the previous subsection, enabling the model to perform NER tasks on the source Domain.

$$\mathcal{L} = - \sum_{t=1}^T \log p(y_t | x_{1:t-1}) \quad (1)$$

where T is the length of the generated sequence, y is the target output, $x_{1:t-1}$ is the input sequence before the current time step t , and $p(y_t | x_{1:t-1})$ is the probability of the model predicting y_t given $x_{1:t-1}$ as input.

However, we aim for the model to focus more on generating better and more accurate responses rather than overly emphasizing the instruction and input. Therefore, the loss during training is computed solely based on the tokens in the model’s response.

$$\mathcal{L}_{source} = - \sum_{t=r}^T \log p(y_t | x_{r:t-1}) \quad (2)$$

where model’s response $x_{res} = \{x_r, x_{r+1}, \dots, x_T\}$.

3.3 Supervised Fine-tuning with contrastive learning

After pre-training on the Source domain, we perform supervised fine-tuning (SFT) on the model using a small number of Target domain samples. Similar to the Source domain, we fine-tune the model with next-token prediction. However, unlike the Source domain, we introduce attention-based contrastive learning during SFT. By constructing positive and negative sample pairs, we optimize entity representations, improve internal attention, and

enhance the model’s perception of entity boundaries. The process of constructing positive and negative sample pairs is as follows:

For a given input x_i and the entity category p_i to be extracted, $q_{i,j}$ represents the entity in x_i . $q_{i,j} \in C_i^{pos}$, $|C_i^{pos}| = J$. Then, $(p_i, q_{i,j})$ forms a positive sample pair, with a total of J pairs. For each positive sample pair $(p_i, q_{i,j})$, we select 2 tokens $n_{i,j,k}$ near the left and right boundary of entity $q_{i,j}$, where $n_{i,j,k} \in C_{i,j}^{neg}$, $|C_{i,j}^{neg}| = 2$, and $(p_i, n_{i,j,k})$ forms a negative sample pair, with a total of 2 pairs. In this way, the model can implicitly learn some information related to entity boundaries. We apply contrastive learning to the model’s attention to improve internal attention, increasing focus on positive samples and reducing focus on negative samples. The contrastive loss function is defined as follows:

$$\begin{aligned} \mathcal{L}_{con} = & - \frac{1}{N} \sum_{i=1}^N \log(\sigma(\sum_j (\mathbf{e}_i^{Q,type} \cdot \mathbf{e}_{i,j}^{K,pos}) \\ & - \sum_k (\mathbf{e}_i^{Q,type} \cdot \mathbf{e}_{i,j,k}^{K,neg}))) \end{aligned} \quad (3)$$

We used cosine similarity to represent the distance between positive and negative sample pairs. Specifically, for a given input x_i , $\mathbf{e}_i^{Q,type}$ represents the embedding of the entity category p_i output by the Q projector in the model. $\mathbf{e}_{i,j}^{K,pos}$ and $\mathbf{e}_{i,j,k}^{K,neg}$ represent the embeddings of the positive sample $q_{i,j}$ and the negative sample $n_{i,j,k}$ output by the K projector, respectively. It is important to note that the output embeddings from both the Q projector head and the K projector head are averaged across all heads and normalized at the 26th layer. Here, we choose the output of the Q and K projector heads instead of the hidden layer states to further improve internal attention and achieve faster convergence and better performance during training.

By combining the SFT loss and the contrastive learning loss, we obtain the overall loss function for fine-tuning the target domain. This allows the model to adapt to the target domain while optimizing the representations’ distribution in the semantic space. Here, λ is used to control the weight of the contrastive learning loss, and in our experiments, $\lambda = 0.01$.

$$\mathcal{L}_{target} = \mathcal{L}_{sft} + \lambda \mathcal{L}_{con} \quad (4)$$

$$\mathcal{L}_{sft} = \mathcal{L}_{source} \quad (5)$$

3.4 Direct Preference Optimization on Entity Boundary

After the initial alignment of the model with the target domain via SFT, we use preference data based on entity boundaries and error feedback to adjust the model’s generation preferences using RLHF. This enables the model to learn more accurate entity boundaries and correct existing errors. The process of constructing preference data is as follows:

(1) Preference Data Based on Entity Boundaries For the data shown in Figure 3, we generate incorrect entity responses by shifting one token left or right from the correct entity boundaries. These incorrect entity responses are labeled as low-preference ‘**rejected**’ samples, while the original correct responses are labeled as high-preference ‘**chosen**’ samples.

chosen: The entities I extracted for you are <<< CTV Television Network >>>.

rejected: The entities I extracted for you are <<< join the CTV Television Network when >>>.

(2) Preference Data Based on Error Feedback We use the training data from the previous phase to test the SFT model that has undergone the first alignment. The misclassified entity extraction results are then used to construct the preference data. Specifically, the original correct answers are labeled as the ‘**chosen**’ data in the preference dataset, while the incorrect responses generated by the SFT model are labeled as the ‘**rejected**’ data.

After constructing the preference data, in traditional RLHF methods, we first need to train a reward model to evaluate and score the generated responses on the preference data $D = \{x^{(i)}, y_w^{(i)}, y_l^{(i)}\}_{i=1}^N$, where $y_w^{(i)}$ and $y_l^{(i)}$ represent the preferred and non-preferred generations given input $x^{(i)}$, respectively. According to the Bradley-Terry (BT) model, the negative log-likelihood loss for the reward model is defined as:

$$\mathcal{L}_R(r_\phi, \mathcal{D}) = -\mathbb{E}_{(x, y_w, y_l) \sim \mathcal{D}} [\log \sigma(r_\phi(x, y_w) - r_\phi(x, y_l))] \quad (6)$$

Where σ is the logistic function, during initialization, $r_\phi(x, y)$ is typically implemented by adding a linear layer on top of the SFT model $\pi^{sft}(y|x)$ from the previous stage to score the model’s generations. After obtaining the trained reward model, the large language model is further optimized based on feedback from the reward model. This process is

formulated as:

$$\max_{\pi_\theta} \mathbb{E}_{x \sim \mathcal{D}, y \sim \pi_\theta(y|x)} [r_\phi(x, y)] - \beta \mathbb{D}_{\text{KL}} [\pi_\theta(y|x) \parallel \pi_{\text{ref}}(y|x)] \quad (7)$$

where β is a parameter controlling the deviation from the baseline reference policy model π_{ref} , $\pi_\theta(y|x)$ is the current language model, and both π_{ref} and $\pi_\theta(y|x)$ are initialized with the SFT model $\pi^{sft}(y|x)$. This ensures that the model is optimized toward higher rewards, as scored by the reward model while preventing the generation distribution from deviating too far from the SFT model, which could otherwise lead to unpredictable and undesirable outputs.

To simplify the training process and avoid the need for training a reward model, we use the Direct Preference Optimization (DPO) method to perform the model policy optimization. Based on the derivation from the Equation 7, we obtain the following:

$$\begin{aligned} & \max_{\pi} \mathbb{E}_{x \sim \mathcal{D}, y \sim \pi} [r(x, y)] - \beta \mathbb{D}_{\text{KL}} [\pi(y|x) \parallel \pi_{\text{ref}}(y|x)] \\ &= \min_{\pi} \mathbb{E}_{x \sim \mathcal{D}} \mathbb{E}_{y \sim \pi(y|x)} \left[\log \frac{\pi(y|x)}{\frac{1}{Z(x)} \pi_{\text{ref}}(y|x) \exp\left(\frac{1}{\beta} r(x, y)\right)} - \log Z(x) \right] \end{aligned} \quad (8)$$

where $Z(x)$ is the partition function. We will not elaborate on the derivation method here. For a detailed derivation, please refer to the paper on DPO (Rafailov et al., 2023).

$$Z(x) = \sum_y \pi_{\text{ref}}(y|x) \exp\left(\frac{1}{\beta} r(x, y)\right) \quad (9)$$

The explicit optimal solution $\pi^*(y|x)$ for model $\pi(y|x)$ is:

$$\pi^*(y|x) = \frac{1}{Z(x)} \pi_{\text{ref}}(y|x) \exp\left(\frac{1}{\beta} r(x, y)\right) \quad (10)$$

The form of the reward model $r(x, y)$ can be derived as follows:

$$r^*(x, y) = \beta \log \frac{\pi^*(y|x)}{\pi_{\text{ref}}(y|x)} + \beta \log Z(x) \quad (11)$$

By substituting the reward model $r(x, y)$ into the loss function under the Bradley-Terry (BT) model Equation 6 for optimization, the optimal solution is directly obtained through the process of training the reward model.

$$\begin{aligned} \mathcal{L}_R(r_\phi, \mathcal{D}) = & -\mathbb{E}_{(x, y_w, y_l) \sim \mathcal{D}} \left[\log \sigma \left(\beta \log \frac{\pi^*(y_1|x)}{\pi_{\text{ref}}(y_1|x)} \right. \right. \\ & \left. \left. - \beta \log \frac{\pi^*(y_2|x)}{\pi_{\text{ref}}(y_2|x)} \right) \right] \end{aligned} \quad (12)$$

Datasets	Domain	#Sent	#Labels
Few-NERD	Mixed	188.2k	66
CoNLL-03	News	20.7k	5
GUM	WiKi	3.5k	12
WNUT-17	Social	5.6k	7
OntoNotes	Mixed	159.6k	19

Table 1: The statistics of each dataset.

The preference generation $y_w^{(i)}$ corresponds to the ‘chosen’ part of the preference data we construct, while the non-preferred generation $y_l^{(i)}$ corresponds to the ‘rejected’ part.

Finally, we incorporate a portion of the model’s SFT loss into the training process to prevent the model from deviating too much from the initial alignment results. α represents the weight of the SFT loss.

$$\mathcal{L}'_{dpo} = \alpha \mathcal{L}_{sft}(\pi^*(y|x)) + \mathcal{L}_{dpo} \quad (13)$$

4 Experiments

4.1 Datasets

We selected two widely used few-shot named entity recognition benchmarks for evaluation: Few-NERD and CrossNER.

Few-NERD: Few-NERD (Ding et al., 2021b) is a large-scale, fine-grained manually annotated NER dataset with 8 coarse-grained and 66 fine-grained entity categories. It provides two few-shot settings: Inter and Intra. In the Inter setting, the training, validation, and test sets share all coarse-grained categories but have disjoint fine-grained entity categories. In the Intra setting, entity categories are disjoint at both coarse-grained and fine-grained levels. Here, we use the episode data released by Ding et al. for experiments, defining the few-shot tasks as N-way K~2K-shot scenarios, where N-way indicates the number of entity categories in the task, and K~2K-shot denotes the sampling of K~2K training instances per entity category.

CrossNER: CrossNER (Hou et al., 2020) consists of four datasets: CoNLL-2003 (Sang and De Meulder, 2003), GUM (Zeldes, 2017), WNUT-17 (Derczynski et al., 2017), and OntoNotes (Pradhan et al., 2013), coming from four distinct domains: News, Wiki, Social, and Mixed. We used the episode data constructed by Hou et al. (2020), selecting two domains for training, one for validation, and one for testing.

4.2 Baselines

For the baselines, we refer to previous works and select several strong methods from both one-stage and two-stage paradigms.

One-stage paradigms include ProtoBERT (Fritzlner et al., 2019), Matching Network (Vinyals et al., 2016), StructShot (Yang and Katiyar, 2020), NNShot (Yang and Katiyar, 2020), CONTAINER (Snigdha et al., 2022), LTapNet+CDT (Hou et al., 2020), Llama3-8b-base(only SFT in target domain), and Llama3-8b(pre+sft).

Two-stage paradigms include ESD (Wang et al., 2022b), DecomMeta (Ma et al., 2022b), SpanProto (Wang et al., 2022a), MSDP (Dong et al., 2023), BANER (Guo et al., 2024).

4.3 Implementation Details

We chose Meta’s Llama3.1-8b (Dubey et al., 2024), available on HuggingFace, as the initial language model. For subsequent training, we employed the LoRA method, fine-tuning only a subset of the large language model’s parameters to reduce hardware requirements. The LoRA rank was set to 8, and the LoRA alpha was set to 16. During the SFT phase, the parameter λ , controlling the contrastive learning loss, was set to 0.01, while in the DPO training phase, the parameter β was set to 0.1, and the weight α for the SFT loss was set to 0.2.

We used Adam as the optimizer and applied different learning rates across training stages: a learning rate of 3e-4 for the source domain pre-training and target domain SFT phases, and 5e-6 for the DPO phase. The warm-up ratio was set to 0.1.

All experiments were conducted using a single 4090 GPU for both training and testing.

4.4 Main Result

Tables 2 and 3 present the main results comparing our method with other baselines. We have the following observations: 1) Our proposed OBP-LLM significantly outperforms previous methods by a large margin on both the Few-NERD and CrossNER benchmarks. Compared to MSDP, it achieves overall average improvements of 2.26% and 17.16% on Few-NERD Inter and Few-NERD Intra, respectively, and a 21.75% improvement on CrossNER, demonstrating the effectiveness of our approach. 2) Among previous methods, two-stage paradigms consistently outperformed one-stage paradigms. However, our method, which preserves the integrity and coherence of the NER task within a one-stage

Paradigms	Models	Intra					Inter				
		1~2-shot		5~10-shot		Avg.	1~2-shot		5~10-shot		Avg.
		5 way	10 way	5way	10 way		5 way	10 way	5way	10 way	
One-stage	ProtoBERT	23.45±0.92	19.76±0.59	41.93±0.55	34.61±0.59	29.94	44.44±0.11	39.09±0.87	58.80±1.42	53.97±0.38	49.08
	NNShot	31.01±1.21	21.88±0.23	35.74±2.36	27.67±1.06	29.08	54.29±0.40	46.98±1.96	50.56±3.33	50.00±0.36	50.46
	StructShot	35.92±0.69	25.38±0.84	38.83±1.72	26.39±2.59	31.63	57.33±0.53	49.46±0.53	57.16±2.09	49.49±1.77	53.34
	CONTaiNER	40.43	33.84	53.70	47.49	43.87	55.95	48.35	61.83	57.12	55.81
	Llama3-8b-base	59.08	55.44	60.38	67.75	60.66	59.13	55.68	75.24	73.43	65.87
	Llama3-8b(pre+sft)	74.24	73.20	75.48	71.90	73.70	77.97	77.23	79.67	77.66	78.13
	OBP-LLM	75.54±2.14	74.31±2.38	78.01±3.11	75.74±2.22	75.90	81.14±4.41	79.23±1.63	81.30±3.79	80.29±2.92	80.49
Two-stage	ESD	41.44±1.16	32.29±1.10	50.68±0.94	42.92±0.75	41.83	66.46±0.49	59.95±0.69	74.14±0.80	67.91±1.41	67.12
	DecomMeta	52.04±0.44	43.50±0.59	63.23±0.45	56.84±0.14	53.9	68.77±0.24	63.26±0.40	71.62±0.16	68.32±0.10	67.99
	SpanProto	54.49±0.39	45.39±0.72	65.89±0.82	59.37±0.47	56.29	73.36±0.18	66.26±0.33	75.19±0.77	70.39±0.63	71.3
	MSDP	56.35±0.28	47.13±0.69	66.80±0.78	64.69±0.51	58.74	76.86±0.22	69.78±0.31	84.78±0.69	81.50±0.71	78.23
	BANER	64.95±0.85	61.24±0.82	72.14±0.33	67.53±0.12	66.47	69.26±0.94	67.43±0.35	76.53±0.51	72.24±0.22	71.37

Table 2: F1 scores on Few-NERD for both inter and intra settings.

Paradigms	Models	1-shot					5-shot				
		CONLL-03	GUM	WNUT-17	OntoNotes	Avg.	CONLL-03	GUM	WNUT-17	OntoNotes	Avg.
One-stage	Matching Network	19.50±0.35	4.73±0.16	17.23±2.75	15.06±1.61	14.13	19.85±0.74	5.58±0.23	6.61±1.75	8.08±0.47	10.03
	ProtoBERT	32.49±2.01	3.89±0.24	10.68±1.40	6.67±0.46	13.43	50.06±1.57	9.54±0.44	17.26±2.65	13.59±1.61	22.61
	L-TapNet+CDT	44.30±3.15	12.04±0.65	20.80±1.06	15.17±1.25	23.08	45.35±2.67	11.65±2.34	23.30±2.80	20.95±2.81	25.31
	Llama3-8b-base	50.14	36.29	40.30	39.07	41.45	60.86	42.28	51.09	54.17	52.10
	Llama3-8b(pre+sft)	55.72	38.15	62.74	53.07	52.42	63.18	49.63	62.17	57.65	58.16
	OBP-LLM	59.55±3.32	44.63±4.78	65.43±3.86	55.31±3.35	56.23	65.67±3.08	51.82±4.41	64.66±2.31	59.81±2.25	60.49
Two-stage	DecomMeta	46.09±0.44	17.54±0.98	25.14±0.24	34.13±0.92	30.73	58.18±0.87	31.36±0.91	31.02±1.28	45.55±0.90	41.53
	SpanProto	47.70±0.49	19.92±0.53	28.31±0.61	36.41±0.73	33.09	61.88±0.83	35.12±0.88	33.94±0.50	48.21±0.89	44.79
	MSDP	49.14±0.52	21.88±0.29	30.10±0.56	38.05±0.88	34.79	63.98±0.80	36.53±0.81	35.61±0.72	49.99±0.95	46.53

Table 3: F1 scores under 1-shot and 5-shot setting on CrossNER.

Methods	Few-NERD		CrossNER	
	Intra	Inter	1-shot	5-shot
OBP-LLM	75.90	80.49	56.23	60.49
w/o contrastive learning	74.56	79.07	53.83	59.23
w/o dpo	75.04	79.56	54.82	59.42

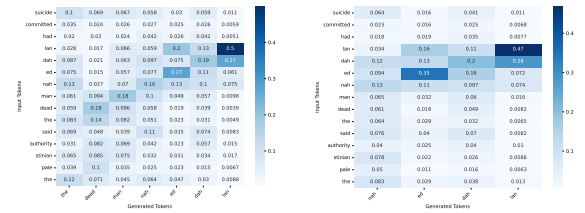
Table 4: The ablation study results (average F1 score) for Few-NERD and CrossNER.

paradigm, is the first to surpass two-stage methods in all aspects. 3) The Intra scenario in Few-NERD is more challenging as entity categories in the training, validation, and test sets are disjoint not only at the fine-grained level but also at the coarse level. Similarly, CrossNER is difficult due to both different entity categories and datasets from diverse domains. Previous methods have significant room for improvement in these tasks. Our OBP-LLM shows remarkable improvements in both Few-NERD and CrossNER, demonstrating its strong generalization ability in few-shot learning, especially in cross-domain scenarios.

4.5 Ablation Study

We conducted ablation studies on the main components of OBP-LLM, focusing on 1) contrastive learning during the SFT phase and 2) Direct Preference Optimization (DPO) based on entity boundary information. The results are shown in Table 4

1) When either of these components is removed, the overall average performance of the model declines, indicating that both components are neces-



(a) base model

(b) with CL

Figure 4: The comparison of attention heatmaps, where (a) represents the Llama3.1-8b model with only SFT training, and (b) represents the model with contrastive learning added during the SFT phase.

sary and highly effective.

2) When contrastive learning is removed, the average F1 score drops by 1.26% to 2.4%, with a more pronounced decline in the cross-dataset task CrossNER. This demonstrates that contrastive learning effectively optimizes the model for cross-domain tasks.

3) When DPO is removed, the average F1 score decreases by approximately 1% overall. Compared to contrastive learning, the drop in F1 score is smaller, as DPO primarily refines the model’s judgment of entity boundaries while maintaining the initial alignment results of the large language model.

4.6 Effectiveness of Contrastive learning

In the SFT phase, we introduce contrastive learning to optimize the distribution of entity representations in the model’s semantic space and enhance its attention mechanism, improving performance

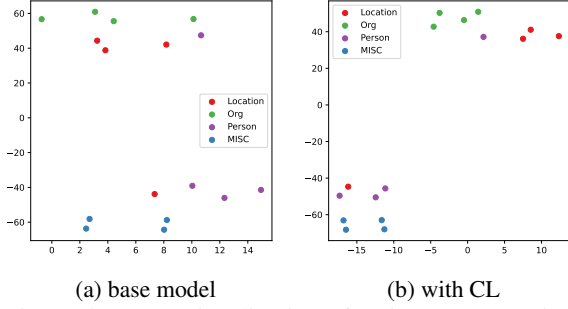


Figure 5: t-SNE visualization of entity representations on CrossNER for the base model and the base model with contrastive learning, with each color representing a different entity category.

in entity recognition tasks.

To evaluate this, we perform SFT on the base Llama3.1-8b model, using it as the baseline. We randomly select some data to test the impact of contrastive learning on attention. As shown in Figure 4, for the standard output “nahed dahlan”, the baseline model attends to irrelevant tokens, resulting in redundant outputs, while contrastive learning helps focus attention on correct entity tokens.

Additionally, we visualized the distribution of entity representations in the semantic space using t-SNE, as shown in Figure 5. Compared to the base model, the model trained with contrastive learning shows a significantly more compact distribution of entities within the same category. However, the improvement in the boundary distinction between different categories of entities was relatively less pronounced. This is because, when constructing negative samples for contrastive learning, to avoid extreme imbalance in the number of positive and negative samples, we selected tokens near the entities rather than all tokens outside the correct entities, many of which are non-entity tokens.

Overall, the results demonstrate that the contrastive learning we introduced effectively improves entity semantic representations and enhances model performance in entity recognition tasks.

4.7 Effectiveness of Direct Preference Optimization

To validate the effectiveness of DPO based on entity boundaries and error feedback, which enhances boundary learning and error correction post-SFT alignment, we randomly sampled 500 instances from the CrossNER task for evaluation. Representative cases are shown in Figure 6. The baseline model, trained only with SFT, often produces redundant words at entity boundaries, which may

Input	the hood opening reminds me of a classic saab 900 _{product} .
Output	saab 900
Baseline	a classic saab 900 ×
Con-DpoNER	saab 900 ✓
Input	are the legality of votes cast by non citizens _{group} checked after they have been cast.
Output	non citizens
Baseline	the legality of votes ×
Con-DpoNER	non citizens ✓

Figure 6: A case of CrossNER. The correct and incorrect entities are highlighted in red and green, respectively.

Dataset	Boundary Error Rate
few-NERD	-10.3%
Cross-NER	-11.69%

Table 5: Quantifying boundary error reduction post-DPO optimization versus SFT-only.

not affect semantics but indicate boundary imprecision. After DPO, the model generates more precise boundaries and corrects earlier errors.

We also tested boundary errors on Few-NERD and CrossNER datasets. As shown in Table 5, DPO optimization reduced boundary errors by 10.3% and 11.69% compared to SFT-only.

5 Conclusion

We propose OBP-LLM, a method for optimizing entity boundary perception in large language models. By introducing attention-based contrastive learning during the SFT phase, we enhance the distribution of entity representations and improve attention, enabling the model to focus on the correct entity tokens. Additionally, we apply RLHF for secondary alignment optimization based on entity boundary information and error feedback, simplifying the training process with DPO. Extensive experiments demonstrate that our approach, requiring only partial parameter training, outperforms previous SOTA baselines, especially in more challenging tasks.

Limitations

As mentioned in Section 4.6, due to the construction method, our model shows limited improvement in distinguishing boundaries between different entity categories in contrastive learning. We believe there is significant room for optimization in the negative sample construction method, which will be a focus of our future research.

References

- Josh Achiam, Steven Adler, Sandhini Agarwal, Lama Ahmad, Ilge Akkaya, Florencia Leoni Aleman, Diogo Almeida, Janko Altschmidt, Sam Altman, Shyamal Anadkat, et al. 2023. Gpt-4 technical report. *arXiv preprint arXiv:2303.08774*.
- Ting Chen, Simon Kornblith, Mohammad Norouzi, and Geoffrey Hinton. 2020. A simple framework for contrastive learning of visual representations. In *International conference on machine learning*, pages 1597–1607. PMLR.
- Paul F Christiano, Jan Leike, Tom Brown, Miljan Martic, Shane Legg, and Dario Amodei. 2017. Deep reinforcement learning from human preferences. *Advances in neural information processing systems*, 30.
- Leon Derczynski, Eric Nichols, Marieke Van Erp, and Nut Limsopatham. 2017. Results of the wnut2017 shared task on novel and emerging entity recognition. In *Proceedings of the 3rd Workshop on Noisy User-generated Text*, pages 140–147.
- Jacob Devlin, Ming-Wei Chang, Kenton Lee, and Kristina Toutanova. 2019. [Bert: Pre-training of deep bidirectional transformers for language understanding](#). In *Proceedings of the 2019 Conference of the North American Chapter of the Association for Computational Linguistics: Human Language Technologies, Volume 1 (Long and Short Papers)*, pages 4171–4186. Association for Computational Linguistics.
- Ning Ding, Guangwei Xu, Yulin Chen, Xiaobin Wang, Xu Han, Pengjun Xie, Haitao Zheng, and Zhiyuan Liu. 2021a. [Few-NERD: A few-shot named entity recognition dataset](#). In *Proceedings of the 59th Annual Meeting of the Association for Computational Linguistics and the 11th International Joint Conference on Natural Language Processing (Volume 1: Long Papers)*, pages 3198–3213, Online. Association for Computational Linguistics.
- Ning Ding, Guangwei Xu, Yulin Chen, Xiaobin Wang, Xu Han, Pengjun Xie, Haitao Zheng, and Zhiyuan Liu. 2021b. Few-nerd: A few-shot named entity recognition dataset. In *Proceedings of the 59th Annual Meeting of the Association for Computational Linguistics and the 11th International Joint Conference on Natural Language Processing (Volume 1: Long Papers)*, pages 3198–3213.
- Guanting Dong, Zechen Wang, Jinxu Zhao, Gang Zhao, Daichi Guo, Dayuan Fu, Tingfeng Hui, Chen Zeng, Keqing He, Xuefeng Li, et al. 2023. A multi-task semantic decomposition framework with task-specific pre-training for few-shot ner. In *Proceedings of the 32nd ACM International Conference on Information and Knowledge Management*, pages 430–440.
- Abhimanyu Dubey, Abhinav Jauhri, Abhinav Pandey, Abhishek Kadian, Ahmad Al-Dahle, Aiesha Letman, Akhil Mathur, Alan Schelten, Amy Yang, Angela Fan, et al. 2024. The llama 3 herd of models. *arXiv preprint arXiv:2407.21783*.
- Alexander Fritzler, Varvara Logacheva, and Maksim Kreto. 2019. Few-shot classification in named entity recognition task. In *Proceedings of the 34th ACM/SIGAPP symposium on applied computing*, pages 993–1000.
- T Gao, X Yao, and Danqi Chen. 2021. Simcse: Simple contrastive learning of sentence embeddings. In *EMNLP 2021-2021 Conference on Empirical Methods in Natural Language Processing, Proceedings*.
- Tianyu Gao, Xu Han, Zhiyuan Liu, and Maosong Sun. 2019. Hybrid attention-based prototypical networks for noisy few-shot relation classification. In *Proceedings of the AAAI conference on artificial intelligence*, volume 33, pages 6407–6414.
- Jiafeng Guo, Gu Xu, Xueqi Cheng, and Hang Li. 2009. [Named entity recognition in query](#). In *Proceedings of the 32nd International ACM SIGIR Conference on Research and Development in Information Retrieval*, pages 267–274, New York, NY, USA. Association for Computing Machinery.
- Quanjiang Guo, Yihong Dong, Ling Tian, Zhao Kang, Yu Zhang, and Sijie Wang. 2024. Baner: Boundary-aware llms for few-shot named entity recognition. *arXiv preprint arXiv:2412.02228*.
- Raia Hadsell, Sumit Chopra, and Yann LeCun. 2006. Dimensionality reduction by learning an invariant mapping. In *2006 IEEE Computer Society Conference on Computer Vision and Pattern Recognition, CVPR 2006*, pages 1735–1742.
- Kaiming He, Haoqi Fan, Yuxin Wu, Saining Xie, and Ross Girshick. 2020. Momentum contrast for unsupervised visual representation learning. In *Proceedings of the IEEE/CVF conference on computer vision and pattern recognition*, pages 9729–9738.
- Yutai Hou, Wanxiang Che, Yongkui Lai, Zhihan Zhou, Yijia Liu, Han Liu, and Ting Liu. 2020. Few-shot slot tagging with collapsed dependency transfer and label-enhanced task-adaptive projection network. In *Proceedings of the 58th Annual Meeting of the Association for Computational Linguistics*, pages 1381–1393.
- Edward J Hu, Yelong Shen, Phillip Wallis, Zeyuan Allen-Zhu, Yanzhi Li, Shean Wang, Lu Wang, and Weizhu Chen. 2021. Lora: Low-rank adaptation of large language models. *arXiv preprint arXiv:2106.09685*.
- Jiaxin Huang, Chunyuan Li, Krishan Subudhi, Damien Jose, Shobana Balakrishnan, Weizhu Chen, Baolin Peng, Jianfeng Gao, and Jiawei Han. 2021. Few-shot named entity recognition: An empirical baseline study. In *2021 Conference on Empirical Methods in Natural Language Processing, EMNLP 2021*, pages 10408–10423. Association for Computational Linguistics (ACL).
- Yinhan Liu, Myle Ott, Naman Goyal, Jingfei Du, Mandar Joshi, Danqi Chen, Omer Levy, Mike Lewis,

695	Luke Zettlemoyer, and Veselin Stoyanov. 2019.	Sarkar Snigdha, Sarathi Das, Arzoo Katiyar, Rebecca J	750
696	Roberta: A robustly optimized bert pretraining ap-	Passonneau, and Rui Zhang. 2022. Container: Few-	751
697	proach . <i>arXiv preprint arXiv:1907.11692</i> .	shot named entity recognition via contrastive learn-	752
698	Jie Ma, Miguel Ballesteros, Srikanth Doss, Rishita	ing. In <i>60th Annual Meeting of the Association</i>	753
699	Anubhai, Sunil Mallya, Yaser Al-Onaizan, and Dan	<i>for Computational Linguistics, ACL 2022</i> , pages	754
700	Roth. 2022a. Label semantics for few shot named	6338–6353. Association for Computational Linguis-	755
701	entity recognition. In <i>Findings of the Association for</i>	tics (ACL).	756
702	<i>Computational Linguistics: ACL 2022</i> , pages 1956–		
703	1971.	Nisan Stiennon, Long Ouyang, Jeffrey Wu, Daniel	757
704	Tingting Ma, Huiqiang Jiang, Qianhui Wu, Tiejun	Ziegler, Ryan Lowe, Chelsea Voss, Alec Radford,	758
705	Zhao, and Chin-Yew Lin. 2022b. Decomposed meta-	Dario Amodei, and Paul F Christiano. 2020. Learn-	759
706	learning for few-shot named entity recognition. In	ing to summarize with human feedback. <i>Advances</i>	760
707	<i>Findings of the Association for Computational Lin-</i>	<i>in Neural Information Processing Systems</i> , 33:3008–	761
708	<i>guistics: ACL 2022</i> , pages 1584–1596.	3021.	762
709	Diego Mollá, Menno Van Zaanen, and Daniel Smith.	Oriol Vinyals, Charles Blundell, Timothy Lillicrap,	763
710	2006. Named entity recognition for question answer-	Daan Wierstra, et al. 2016. Matching networks for	764
711	ing . In <i>Proceedings of the Australasian Language</i>	one shot learning. <i>Advances in neural information</i>	765
712	<i>Technology Workshop 2006</i> , pages 51–58.	<i>processing systems</i> , 29.	766
713	David Nadeau and Satoshi Sekine. 2007. A survey of	Jianing Wang, Chengyu Wang, Chuanqi Tan, Minghui	767
714	named entity recognition and classification . <i>Lingvis-</i>	Qiu, Songfang Huang, Jun Huang, and Ming Gao.	768
715	<i>ticae Investigationes</i> , 30(1):3–26.	2022a. Spanproto: A two-stage span-based prototyp-	769
716	Long Ouyang, Jeffrey Wu, Xu Jiang, Diogo Almeida,	ical network for few-shot named entity recognition.	770
717	Carroll Wainwright, Pamela Mishkin, Chong Zhang,	In <i>Proceedings of the 2022 Conference on Empiri-</i>	771
718	Sandhini Agarwal, Katarina Slama, Alex Ray, et al.	<i>cal Methods in Natural Language Processing</i> , pages	772
719	2022. Training language models to follow instruc-	3466–3476.	773
720	tions with human feedback. <i>Advances in neural in-</i>	Peiyi Wang, Runxin Xu, Tianyu Liu, Qingyu Zhou,	774
721	<i>formation processing systems</i> , 35:27730–27744.	Yunbo Cao, Baobao Chang, and Zhifang Sui. 2022b.	775
722	Sameer Pradhan, Alessandro Moschitti, Nianwen Xue,	An enhanced span-based decomposition method for	776
723	Hwee Tou Ng, Anders Björkelund, Olga Uryupina,	few-shot sequence labeling. In <i>Proceedings of the</i>	777
724	Yuchen Zhang, and Zhi Zhong. 2013. Towards robust	<i>2022 Conference of the North American Chapter of</i>	778
725	linguistic analysis using ontonotes. In <i>Proceedings</i>	<i>of the Association for Computational Linguistics: Hu-</i>	779
726	<i>of the Seventeenth Conference on Computational Nat-</i>	<i>man Language Technologies</i> , pages 5012–5024.	780
727	<i>ural Language Learning</i> , pages 143–152.	Shuhe Wang, Xiaofei Sun, Xiaoya Li, Rongbin Ouyang,	781
728	Rafael Rafailov, Archit Sharma, Eric Mitchell, Stefano	Fei Wu, Tianwei Zhang, Jiwei Li, and Guoyin Wang.	782
729	Ermon, Christopher D Manning, and Chelsea Finn.	2023. Gpt-ner: Named entity recognition via large	783
730	2023. Direct preference optimization: your language	language models. <i>arXiv preprint arXiv:2304.10428</i> .	784
731	model is secretly a reward model. In <i>Proceedings of</i>	Yi Yang and Arzoo Katiyar. 2020. Simple and effective	785
732	<i>the 37th International Conference on Neural Inform-</i>	few-shot named entity recognition with structured	786
733	<i>ation Processing Systems</i> , pages 53728–53741.	nearest neighbor learning. In <i>Proceedings of the</i>	787
734	N Reimers. 2019. Sentence-bert: Sentence embed-	<i>2020 Conference on Empirical Methods in Natural</i>	788
735	dings using siamese bert-networks. <i>arXiv preprint</i>	<i>Language Processing (EMNLP)</i> , pages 6365–6375.	789
736	<i>arXiv:1908.10084</i> .	Amir Zeldes. 2017. The gum corpus: Creating mul-	790
737	Erik Tjong Kim Sang and Fien De Meulder. 2003. In-	tilayer resources in the classroom. <i>Language Re-</i>	791
738	troductio to the conll-2003 shared task: Language-	<i>sources and Evaluation</i> , 51(3):581–612.	792
739	independent named entity recognition. In <i>Proceeed-</i>	Yafeng Zhang, Zilan Yu, Yuang Huang, and Jing Tang.	793
740	<i>ings of the Seventh Conference on Natural Language</i>	2024. Cllmfs: A contrastive learning enhanced large	794
741	<i>Learning at HLT-NAACL 2003</i> , pages 142–147.	language model framework for few-shot named entity	795
742	Yongliang Shen, Xinyin Ma, Zeqi Tan, Shuai Zhang,	recognition. In <i>ECAI 2024</i> , pages 1985–1992. IOS	796
743	Wen Wang, and Weiming Lu. 2021. Locate and la-	Press.	797
744	bel: A two-stage identifier for nested named entity	Xingyu Zhu, Feifei Dai, Xiaoyan Gu, Bo Li,	798
745	recognition. In <i>Proceedings of the 59th Annual Meet-</i>	Meiou Zhang, and Weiping Wang. 2024. G1-ner:	799
746	<i>ing of the Association for Computational Linguistics</i>	Generation-aware large language models for few-shot	800
747	<i>and the 11th International Joint Conference on Natu-</i>	named entity recognition. In <i>International Confer-</i>	801
748	<i>ral Language Processing (Volume 1: Long Papers)</i> ,	<i>ence on Artificial Neural Networks</i> , pages 433–448.	802
749	pages 2782–2794.	Springer.	803

804 Daniel M Ziegler, Nisan Stiennon, Jeffrey Wu, Tom B
805 Brown, Alec Radford, Dario Amodei, Paul Chris-
806 tiano, and Geoffrey Irving. 2019. Fine-tuning lan-
807 guage models from human preferences. *arXiv*
808 *preprint arXiv:1909.08593*.